




A Biologically-Inspired Appearance Model for Snake Skin

Juan Raul Padron-Griffe , Diego Bielsa, Adrian Jarabo  and Adolfo Muñoz 

Universidad de Zaragoza - I3A

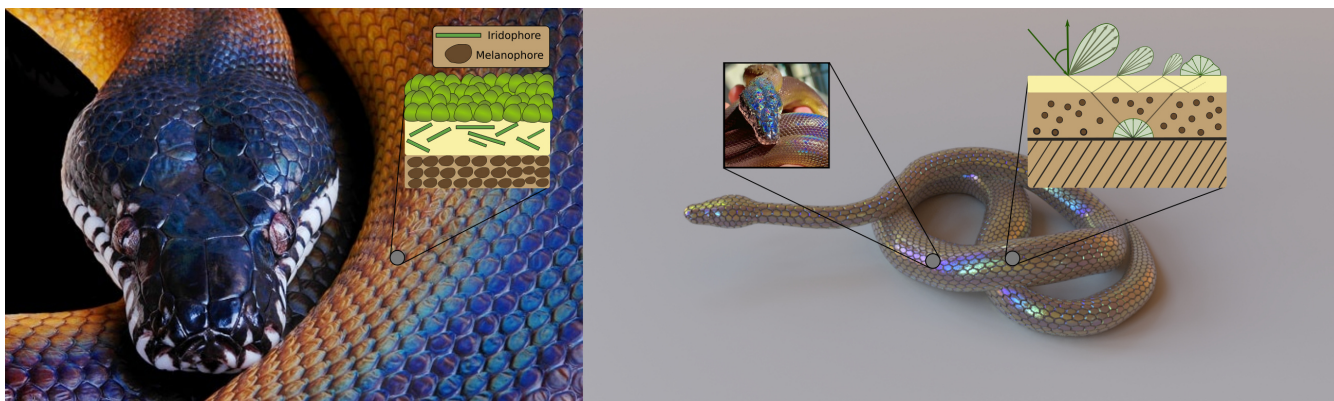


Figure 1: *Left:* Real photograph of a white lipped python [sta20]. A reptile scale is a biological tissue composed of multiple layers of chromatophores (see right inset) like irodophores (platelets) and melanophores (irregular ellipses). *Right:* A rendering of a snake 3D model using our practical reptile skin reflectance model roughly matching the general appearance. The snake skin is represented as a multilayered material with two layers (right inset): a thin film layer responsible of the iridescent patterns and a diffuse substrate surrounded by an absorbing media responsible of the darkening of the final appearance.

Abstract

Simulating the light transport on biological tissues is a longstanding challenge, given its complex multilayered structure. In biology, one of the most remarkable and studied examples of tissues are the scales that cover the skin of reptiles, which present a combination of photonic structures and pigmentation. This is, however, a somewhat ignored problem in computer graphics. In this work, we propose a multilayered appearance model based on the anatomy of the snake skin. Some snakes are known for their striking, highly iridescent scales resulting from light interference. We model snake skin as a two-layered reflectance function: The top layer is a thin layer resulting on a specular iridescent reflection, while the bottom layer is a diffuse highly-absorbing layer, that results into a dark diffuse appearance that maximizes the iridescent color of the skin. We demonstrate our layered material on a wide range of appearances, and show that our model is able to qualitatively match the appearance of snake skin.

1. Introduction

Photo-realistic rendering of biological tissues and structures, like feathers, fur or reptile skin, is still an open problem. The structural complexity at multiple scales of these biological elements result into complex light-matter interactions, manifested as intriguing appearances at macroscopic scale. One of the most remarkable and studied examples of biological tissues are the scales that cover the skin of reptiles, which present a combination of photonic structures and pigmentation.

Unfortunately, current appearance models in computer graphics mostly ignore the complex anatomic structure of scales and its coloration mechanisms. In general, these appearances are modeled using time-consuming appearance matching by skilled artists. This limits the applicability of computer generated images in areas beyond movies and videogames, such as predictive rendering in paleontology [MMS12, MOK*16], meta-material prototyping, or data-generation for machine learning. In these fields, a predictive physically-grounded appearance model is a must.

In this work, we propose a practical biophysically-inspired ap-

© 2023 The Authors.

Proceedings published by Eurographics - The European Association for Computer Graphics.

This is an open access article under the terms of the Creative Commons Attribution License, which permits use, distribution and reproduction in any medium, provided the original work is properly cited.

pearance model for the skin of snakes. Skin snakes present a wide range of appearances, from simple diffuse ones to highly iridescent. Such complex appearance is the result of the underlying structure of reptile skin, roughly divided in three parallel layers: The first layer is like a platelet-like photonic glass responsible of iridiscense, the second layer is a purely absorbing layer due to the concentration of melanophores, and the bottom layer is a diffuse layer (see the layered material inset Fig.1)

We build our model on top of the position-free model proposed by Guo et al. [GHZ18], where the top layer is modeled as a thin-film with parametrizable height, and the bottom absorbing layer accounts for both volumetric absorption and diffuse surface reflection. Then we demonstrate that our model is able to predict the appearance on real-world snakes, generalizes to other appearances, and it is practical and easy to incorporate in any RGB physically-based renderer.

2. Related Work

The complexity of real-world appearance is in part due to its underlying layered structure and the optical mechanisms involved in its coloration and scattering. Here we review the most relevant works related to our model, and refer the reader to other sources for a broader survey [FJM*20].

Biologically-inspired appearance models The modeling of biological models is not new in graphics, though most existing works have focused on accurately representing human skin [DJ05, DWd*08, IGAJG15] or hair [MJC*03, HHH22]. Other works have generalized hair to other keratin-based structures including fur [YTJR15], feathers [HMC*22], or the Morpho butterfly wings [Sun06]. Closest to ours, Dhillon et al. [DTS*14] modeled snake-skin surface appearances accounting for the diffraction due to grating-like photonic nanostructures in the scales. Later, Dhillon and Ghosh [DG16] proposed a Chebyshev approximation in order to reduce the runtime memory footprint of the surface nanostructure's lookup tables obtained by atomic force microscopy. However, their model requires capturing the surface nanostructure and performing a Fourier transform of the resulting height field, making the approach expensive and difficult to generalize. In contrast, our model simplifies the photonic behaviour of the skin by means of an easy-to-parametrize thin layer, making it easy to author and practical in render time.

Volumetric materials Light transport simulations of volumetric materials typically consists of solving the radiative transfer equation (RTE) [Cha60], and its generalizations to anisotropic [JAM*10] and non-exponential [BRM*18, JAG18] media. We refer the reader to [NGH*18] for more details. In our work, we model the dark appearances of the reptile skin with a diffuse subtract surrounded with an homogeneous absorbing media.

Wave optics-aware appearance models Wave optics phenomena generally manifests in two main phenomena: Diffraction and thin-film interference. Diffraction accounts for the Huygens principle, and it is generally based on the first-order Born approximation (the Kirschhoff equation) [GMN94, Sta99, CHB*12, YHW*18, FJF20].

A particular case of wave-phenomena occurs in thin films, where interference between light paths of different path length result into colorful appearance. These works are the basis for Sun et al. [Sun06] and Dhillon et al.'s [DTS*14] Morpho butterfly and snake skin models, respectively. On the other hand, Smits and Meyer [SM92] introduced the first model accounting for such thin film. More recently, Belcour and Barla [BB17] extended the micro-facet model to account for thin-film interfaces. This approach was leveraged by Huang et al. [HMC*22] to represent the iridescent appearance of the rock dove neck feathers, while pearlescent materials [GMG*20] are generally modeled by embedding thin-film platelets inside a clear media. In this paper, we leverage thin-film interference to model the iridescent appearance of snake skin.

Layered Materials Hanrahan and Kruger [HK93] introduced the first analytical single scattering model for layered materials. Donner and Jensen [DJ05] developed a significantly faster solution for diffuse materials based on the multipole diffusion approximation. A similar approach was followed by Jakob et al. [JdJM14], and later Zeltner and Jakob [ZJ18], generalizing it to materials with any scattering frequency. However, these works require pre-computation and significant storage. A more practical approach was the approximation by Weidlich and Wilkie [WW07] which represented each layer by using multiple BSDF lobes (one for each layer), by introducing several approximation and ignoring multiple scattering. Belcour [Bel18]'s model followed a similar approach, but was able to account for multiple scattering and more complex phenomena. The most general approach is the one by Guo et al. [GHZ18], which leverages the position-free nature of BSDFs, and solves their appearance by using multiple importance sampling of bidirectional Monte Carlo paths inside the stacked volumes. We use this formulation in this work to efficiently compute the light transport simulation of our multilayered reptile skin material.

3. Background

In nature, colours can be produced by pigments selectively absorbing some wavelengths of light, or by constructive and destructive wave interference on (partially) ordered structures at micro- and nacosopic scale (structural coloration), or a combination of both mechanisms [SD17]. Some spectacular examples of structural coloration are the brilliant blue color in the wings of Morpho butterflies, the metallic reflection from the Japanese jewel beetles' wings, or the highly iridescent colors of the peacock feathers [Yos05]. In reptiles, and more particularly in snakes, structural coloration can be found, for example, in the scales of the *Xenopeltis unicolor* snake. In this work, we are interested in snake scales, and in particular on how the epidermis structure and material properties of the skin affect the appearance at macroscopic scale. In the following, we first describe the anatomy of the snake skin; then, we briefly describe thin-film interference, a structural coloration phenomenon we leverage in this work.

3.1. Snake skin anatomy

The snake skin exhibits features that are structurally different from other living beings, in particular its scales and underlying skin layers. At a macroscopic level, the most relevant aspect for appearance

is the scales pattern. There is a wide range of patterns depending on the different snake species.

At a micro-structure level, the skin is divided in multiple roughly parallel layers (Fig. 3a), where the most relevant for appearance is the outermost epidermis layer (the *oberhäutchen*). This layer can also be divided in multiple sublayers, as shown in Fig. 3b. While scanning electron microscopy (SEM) of skin cross sections [KG12, Aya22] reveal a significant variation in the epidermis structure between species, most light interactions occur at the outermost layer. At the top of this *oberhäutchen* we can find the *iridophores*, which is a photonic structure made of small thin platelets, which interact with light as small thin-film elements. Depending on whether these iridophores are ordered or not, they result into more or less visible iridescence. Below these iridophores there is a dark pigment layer, dominated mostly by eumelanin. This layer of pigments can be divided into two layers: the top one is a pigmented layer with disordered melanocytes that absorb light, while the bottom one is a soft tissue that acts as a diffuse reflector.

3.2. Thin-film interference

The iridophores inside the *oberhäutchen* produce iridescence by a mechanism generally called *thin-film interference*. Thin-film interference is the result of multiple reflections inside a parallel dielectric film, of thickness in the order of the visible light wavelength.

Let us consider a parallel thin film with thickness δ and index of refraction (IOR) η_1 , between two media with IOR η_0 on the top and η_2 on the bottom. As an incident light with wavelength λ and incidence angle θ interacts with the dielectric thin, it might be either reflected or refracted following the Fresnel equations. When transmitted inside the thin film, light might suffer several reflections inside it before it is transmitted back, either from the top to the medium with IOR η_0 or the bottom to the medium with IOR η_2 (see Fig. 2, left). Everytime it interacts with the surface of the film, light is attenuated by the Fresnel term by a factor $r_{i|j} = \text{Fresnel}(\theta, \eta_i, \eta_j)$ if reflected at the interface between media with IOR η_i and η_j respectively, or $t_{i|j} = 1 - r_{i|j}$ if transmitted. In addition, as light travels inside the thin film, it suffers a phase delay proportional to the traveled distance.

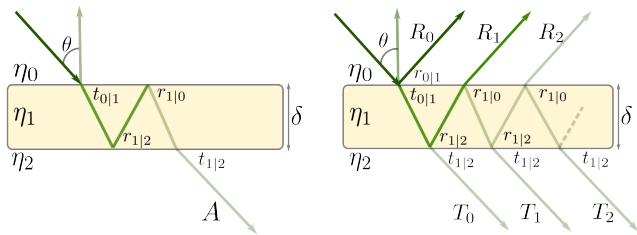


Figure 2: Illustration of the optical path length difference for light reflected from the upper and lower boundaries of a thin-film interference. **Left:** A particular light path, where $r_{i|j}$ and $t_{i|j}$ denotes the amplitude of the reflection and transmission from layer i to layer j . **Right:** General scenario for a single thin-film scenario. The dashed lines implies the path continues indefinitely.

As light emerges from the thin film, either from the top (reflection term R) or the bottom (transmission term T) with different phases depending on the traveled optical depth (see Fig. 2, right), it might interact constructively or destructively, and this interference is dependent on the light's wavelength λ . This results in a rainbow-like color, which is dependent on the angle of incidence.

Assuming that the IOR of the thin film η_1 is real (there is no absorption inside the thin film), we can compute the total reflected energy I_R using the Airy approximation, as

$$I_R(\lambda, \theta) = \left(\frac{n_2 \cos \theta_2}{n_0 \cos \theta_0} \right) \frac{|t_{0|1} t_{1|2}|^2}{|r_{1|0} r_{1|2}|^2 - 2r_{1|0} r_{1|2} \cos \phi + 1}, \quad (1)$$

with ϕ the phase delay between two consecutive reflected paths, computed as

$$\phi = \frac{4\pi}{\lambda} \eta_1 \delta \cos(\theta_1) + \Delta, \quad (2)$$

with θ_1 the refracted angle in the thin-film layer, and Δ the phase change due to Fresnel interaction, computed as

$$\Delta_{i|j} = \begin{cases} 0 & \text{if } \eta_i > \eta_j, \\ \pi & \text{if } \eta_i < \eta_j. \end{cases} \quad (3)$$

Similarly, we can compute the transmitted energy I_T as $I_T(\lambda, \theta) = 1 - I_R(\lambda, \theta)$. A thorough derivation of this formula can be found in multiple sources (e.g. [Yeh05]).

4. Our Model

We model the appearance of snakes skin using a multilayered BSDF that represents the outermost *oberhäutchen*. The first layer reproduces the iridescent effects via thin-film interference (Section 4.2). The second layer consists of a diffuse surface surrounded by an absorbing media, modeling the darkening and saturation of the final appearance (Section 4.3). Our model is summarized in Fig. 3c, while the parameters of our model can be found in Table 1.

Parameter	Definition
δ_0	thickness of the thin film layer (nm)
η_0	refractive index of the top layer
η_1	refractive index of the intermediate layer
η_2	refractive index of the bottom layer
σ_a	absorption coefficient of the absorbing media
δ_1	thickness of the absorbing media layer (nm)
k_d	albedo of the diffuse surface

Table 1: Parameters used in our BSDF. The thickness of the layers are given in nanometers. We set $\eta_0 = 1.0$ and $\eta_1 = 1.53$ to the air and keratin IOR respectively.

4.1. Scales mesogeometry

We model the scales of the snake skin as a mesogeometry, using a tileable bump mapping. In our examples, we simulate the scales of the *Xenopeltis unicolor*, which roughly follow a uniform hexagonal grid, as shown in Fig. 4a. In our case, we manually create the bump map texture; creating a procedural model similar to Voronoi cells of a blue noise distribution of points for the skin's scales is left as future work.

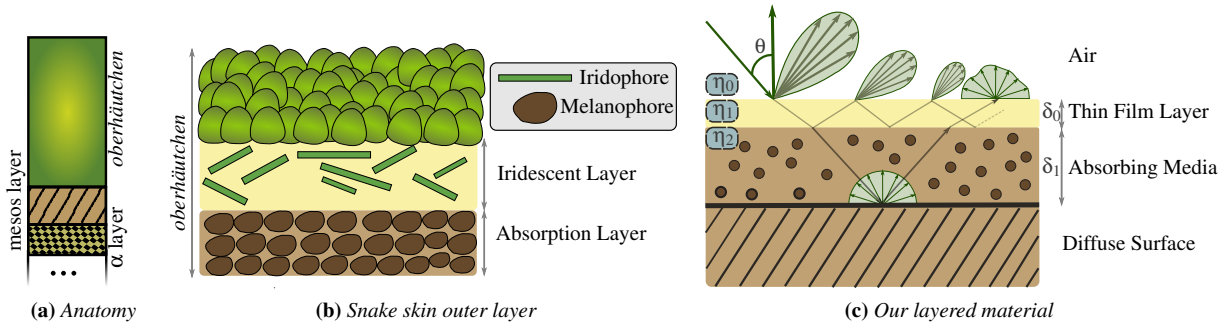


Figure 3: Illustration of the multilayered model for snake skin. (a) A sketch of the snake skin anatomy, which is, essentially multilayered. (b) The outer layer of the snake skin is fundamental for the appearance, as it contains different types of chromatophores. (c) Our multilayered material representation is composed of a thin-film layer responsible of the iridescent effects and a diffuse substrate surrounded by an absorbing media mimicking the appearance of the melanophores' layer.

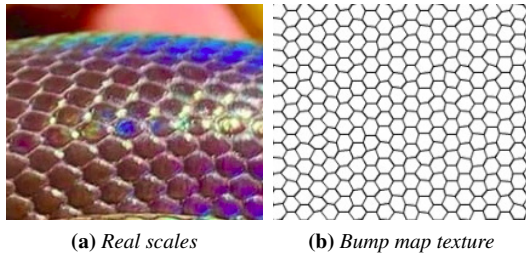


Figure 4: Modelling snake scales as a bump map. **Left:** Prominent iridescent scales from a *Xenopeltis Unicolor* (close-up photography [9GA20]). **Right:** The scale patterns can be faithfully approximated by a hexagonal grid texture.

4.2. Iridescent layer

The outermost layer in the skin of snakes is the so-called iridescent layer, which is a dielectric non-absorbing layer with a quasi-regular photonic structure consisting of several (potentially oriented) iridescent platelets (see Section 3). While volumetric models in the spirit of Guillén et al.'s [GMG*20] could be used for modeling this layer, we opted for a simpler approximation at the cost of potentially reducing our model expressivity.

We assume that the aggregated effect of the platelets can be approximated well by a single thin iridescent layer, following the Airy reflectance described in (1) (and its analogous for transmittance). Thus, we model the reflectance and transmission of this first layer as the BSDF

$$f_0(\omega_i, \omega_o) = \text{DiracDelta}(\omega_o - \omega_r) I_R(\theta) \quad (4)$$

$$+ \text{DiracDelta}(\omega_o + \omega_i)(1 - I_R(\theta)), \quad (5)$$

with ω_r the reflected direction. For clarity, we omit the wavelength dependency of the BSDF.

This approximation has been shown to be very accurate for oriented platelets [BB17], and assuming a fixed IOR allows for changing the appearance of the skin by using a single parameter (the

layer thickness), instead of the multiple parameters required by the model of Guillén et al.

4.3. Absorbing layer

The second layer in our model is an absorbing diffuse layer, modeling the dielectric volumetric layer with melanosomes in snake skin, and the diffuse reflector behind that volumetric layer. As mentioned before, a pigmented layer behind the iridescent layer is crucial for enhancing the structural coloration of snakes.

We model the absorbing layer using the classical Beer-Lambert exponential transmittance, on top of a diffuse reflector. For quick evaluation, we combined these two effects together in a single BRDF as follows

$$f_1(\omega_i, \omega_o) = \frac{k_d}{\pi} e^{-\sigma_a \frac{\delta_1}{|\mathbf{n} \cdot \omega_i| |\mathbf{n} \cdot \omega_o|}}, \quad (6)$$

with k_d the albedo of the diffuse surface, σ_a and δ_1 are the absorption coefficient thickness of the absorbing layer, and \mathbf{n} the normal of the surface.

4.4. Implementation

We implemented our reflectance model as a BSDF plugin in Mitsuba [Jak14], on top of the position-free Monte Carlo (PFMC) framework of Guo et al. [GHZ18]. It allow us to easily compute the multiple interactions between the iridescent and absorbing layer, by explicitly modeling the light transport inside the multilayered material. PFMC assumes that each layer is horizontally infinite, which allows to remove the horizontal position at the layered material, which is crucial for performing next-event estimation under smooth dielectric boundaries. We also leverage the bidirectional multiple importance sampling estimator in PFMC for further reduce variance when evaluating and sampling our model.

Despite the wavelength dependency of thin-film-based iridescence, we opt for a traditional RGB rendering pipeline, using three representative wavelengths for the computations roughly representing RGB (650, 510 and 475 nm, respectively). While this is prone to

spectral aliasing [BB17] we found that the results were reasonable, and made our implementation and integration in Mitsuba simpler.

5. Analysis and results

We now present the evaluation of our method, which consist of an ablation study of our final appearance model and appearance range analysis of our thin film materials. Next, we perform a performance study, where we compare the rendering time for different image resolutions and composition.

5.1. Validation

We validate our model qualitatively by comparing renders with real photographs of the *Xenopeltis unicolor* snake. The renderings were obtained by creating a similar scene in Mitsuba, where the snake geometry and texture scales coarsely matched the snake. As shown in Fig. 1 our renders qualitatively match the general appearance of the photographs under comparable lighting and viewing conditions. Please notice the similarity of the iridescent patterns.

5.2. Appearance Analysis

We first demonstrate our model by exploring the range of appearances that our model is able to generate. Fig. 5 shows the results of this study: We fix the index of refraction of the top layer and intermediate layer to $\eta_0 = 1$ (air) and $\eta_1 = 1.56$ (keratin), respectively, and render a snake scene varying the thickness of the thin film layer δ_0 (rows) and the refraction index of the bottom layer η_2 (column). As we can see in the figure, the appearance changes drastically in both scenarios.

5.3. Ablation studies

In Fig. 6 we analyze the contribution of each component of our appearance to the final overall appearance. In addition to the snake model, we also leverage two additional geometries (a sphere and a toroid). We demonstrate the importance of the mesoscopic bump-based detail, the iridescent layer, and the bottom absorbing layer. This ablation study shows that each component of our appearance model is indeed important for the final appearance.

5.4. Performance

We create all our renders using the position-free Monte Carlo integrator in Mitsuba 0.6 on an Intel Core i9-10900KF CPU with 20 cores. A render of a 3D snake geometry with 1024 spp takes 3.1 min and 7.5 min for HD (1280 × 720) and full HD (1920 × 1080) image resolutions respectively. We report the rendering time in Table 2 on the same machine for our ablation studies experiment. Our multi-layer material is only 1.5 times slower than a traditional diffuse material.

6. Discussion and Conclusion

We have introduced a practical reflectance model for efficient rendering of skin of snakes. Our appearance model is built as a multilayered material composed of two layers: The irodophores layer

Fig.	Time (sphere)	Time (torus)	Time (snake)
6 (a)	2.3 min	2.6 min	2.5 min
6 (b)	2.3 min	2.6 min	2.6 min
6 (c)	3.1 min	3.5 min	3.5 min
6 (d)	4.5 min	4.0 min	3.5 min

Table 2: Rendering time for our ablation studies (Fig. 6) using 1024 spp and a HD image resolution (1280 × 720).

(top layer) responsible of the highly iridescent colors is represented as a thin-film layer, while the bottom layer responsible for the dark pigments is modelled as a diffuse substrate surrounded by an absorbing media. We verify visually that our appearance model can qualitatively match the appearance of a real snake (the *Xenopeltis unicolor*).

Limitations and future work Our model is based on several assumptions, which allows a practical and easy to integrate model, but that departs slightly from the real phenomena in the skin of snakes. First of all, our model is based on the BSDF, and ignores all non-local effects existing in organic materials due to subsurface scattering. However, given the structure of the snake skin, where most of the appearance is dominated by specular reflection in the epidermis, is reasonable to think that translucency will likely play a minor role in appearance.

The second approximation is on the iridescent layer: As discussed above, we simplify the modeling of the layer as a simple global thin-layer on top of a diffuser. This is practical and efficient, but a coarse simplification of the actual structure. Including a platelet-based iridescent model, potentially with a distribution of platelets orientation, might likely increase the expressivity of our model, at the cost of making it more expensive.

Additionally, while our structural coloration model (thin-film interference) is one of the main sources of structural coloration, others such as diffraction gratings due to regular nanoscopic structure of the epidermis [DTS*14] have been omitted in our case. Nevertheless, we have shown how thin-film interference provides a versatile and expressive tool, that is very efficient and suitable for multilayered material representations (as opposed to diffraction gratings) and provides a wide range of snake skin appearances. In terms of parameter tuning, our appearance model is more compact and practical as the final appearance is only defined with 7 global parameters (see Table 1) and it does not require measured data by a complex capture process neither an expensive precomputation.. Finding a practical way to include surface grating nanostructures to our appearance model might be one step closer to the underlying physical light transport happening at reptile skin.

Finally, the light transport itself is rather limited in our renders, reducing light interactions to tristimulus ray-optics-based models. Generalizing our model to account for the full spectrum is trivial. Including more advanced light transport effects, such as the effect of coherence [SY21] in a physical light transport simulation would require additional development, but would bring our model closer to an actually-predictive simulation of appearance.

Our appearance model is potentially capable of generating a

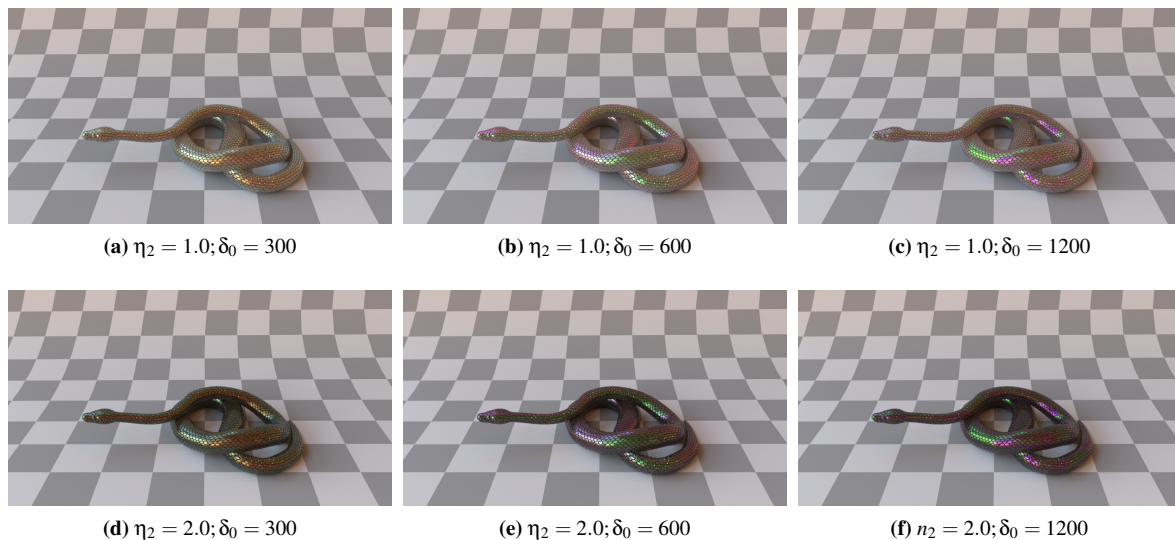


Figure 5: Appearance range study of our thin-film layer. Default parameters: thin-film layer ($\eta_0 = 1$ and $\eta_1 = 1.56$), absorption layer ($\sigma_a = 0.7$, $\delta_1 = 2$ nm, $k_d = 0$). **Top:** varying the thickness of the thin film layer; **Bottom:** varying the index of refraction of the bottom layer η_2 .

wide range of appearances. Nevertheless, only a relatively small subset corresponds to real snakes' appearances. Exploring a wider range of snakes, as well as a broader set of reptiles and fishes that present comparable structure in their skin, is an interesting avenue of future work.

Acknowledgements

The authors would like to thank the anonymous reviewers for their time and insightful comments, and Dario Lanza for his help with the figures. This project has received funding from the European Union's Horizon 2020 research and innovation programme under the Marie Skłodowska-Curie grant agreement No 956585 (PRIME). The work was also partially funded by MCIN/AEI 10.13039/501100011033 through Project PID2019-105004GB-I00.

References

- [9GA20] 9GAGGER: Iridescent sunbeam snakes, 2020. 4
- [Aya22] AYAZ M. Y. B. D.: Hierarchical microstructure of the scales in grass snake (matrix matrix) and dice snake (matrix tessellata). 3
- [BB17] BELCOUR L., BARLA P.: A Practical Extension to Microfacet Theory for the Modeling of Varying Iridescence. *ACM Transactions on Graphics* 36, 4 (July 2017), 65. 2, 4, 5
- [Bel18] BELCOUR L.: Efficient rendering of layered materials using an atomic decomposition with statistical operators. *ACM Trans. Graph.* 37, 4 (jul 2018). 2
- [BRM*18] BITTERLI B., RAVICHANDRAN S., MÜLLER T., WRENNINGE M., NOVÁK J., MARSCHNER S., JAROSZ W.: A radiative transfer framework for non-exponential media. *ACM Trans. Graph.* 37, 6 (dec 2018). 2
- [Cha60] CHANDRASEKHAR S.: *Radiative Transfer*. Dover Publications, London, 1960. 2
- [CHB*12] CUYPERS T., HABER T., BEKAERT P., OH S. B., RASKAR R.: Reflectance model for diffraction. *ACM Transactions on Graphics (TOG)* 31, 5 (2012), 1–11. 2
- [DG16] DHILLON D. S. J., GHOSH A.: Efficient surface diffraction renderings with chebyshev approximations. In *SIGGRAPH ASIA 2016 Technical Briefs* (New York, NY, USA, 2016), SA '16, Association for Computing Machinery. 2
- [DJ05] DONNER C., JENSEN H. W.: Light diffusion in multi-layered translucent materials. *ACM Trans. Graph.* 24, 3 (jul 2005), 1032–1039. 2
- [DTS*14] DHILLON D., TEYSSIER J., SINGLE M., GAPONENKO I., MILINKOVITCH M., ZWICKER M.: Interactive diffraction from biological nanostructures. *Computer Graphics Forum* 33, 8 (2014), 177–188. 2, 5
- [DWd*08] DONNER C., WEYRICH T., D'EON E., RAMAMOORTHY R., RUSINKIEWICZ S.: A layered, heterogeneous reflectance model for acquiring and rendering human skin. *ACM transactions on graphics (TOG)* 27, 5 (2008), 1–12. 2
- [FJF20] FALSTER V., JARABO A., FRISVAD J. R.: Computing the bidirectional scattering of a microstructure using scalar diffraction theory and path tracing. *Computer Graphics Forum* 39, 7 (2020), 231–242. 2
- [FJM*20] FRISVAD J. R., JENSEN S. A., MADSEN J. S., CORREIA A., YANG L., GREGERSEN S. K. S., MEURET Y., HANSEN P.-E.: Survey of models for acquiring the optical properties of translucent materials. *Computer Graphics Forum* 39, 2 (2020), 729–755. 2
- [GHZ18] GUO Y., HAŠAN M., ZHAO S.: Position-free monte carlo simulation for arbitrary layered bsdfs. *ACM Trans. Graph.* 37, 6 (dec 2018). 2, 4
- [GMG*20] GUILLÉN I., MARCO J., GUTIERREZ D., JAKOB W., JARABO A.: A general framework for pearlescent materials. *ACM Transactions on Graphics* 39, 6 (2020). 2, 4
- [GMN94] GONDEK J. S., MEYER G. W., NEWMAN J. G.: Wavelength dependent reflectance functions. In *Proceedings of the 21st Annual Conference on Computer Graphics and Interactive Techniques* (New York, NY, USA, 1994), SIGGRAPH '94, Association for Computing Machinery, p. 213–220. 2

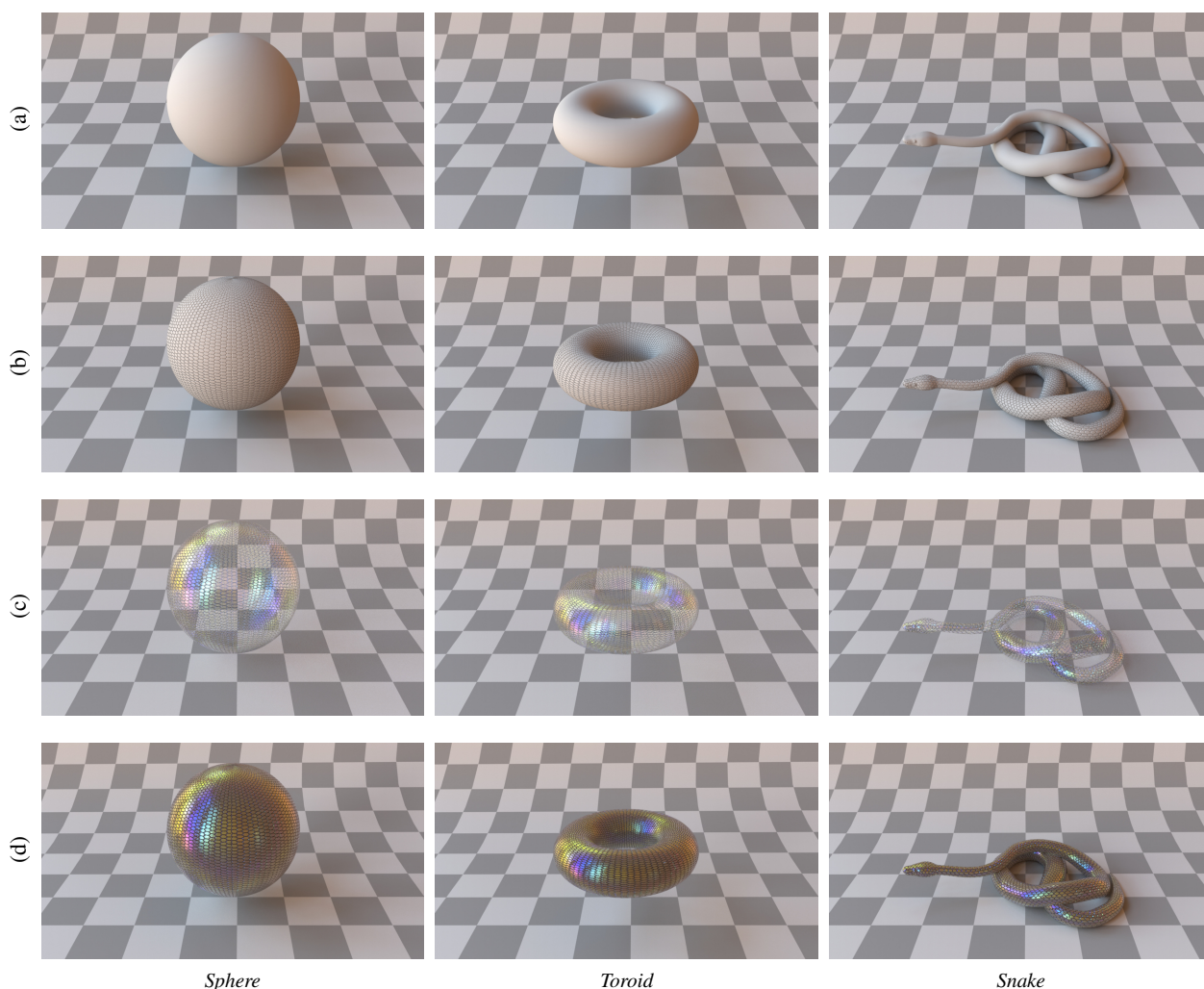


Figure 6: Ablation studies of our BSDF model for reptile skin. (a) Geometric models with diffuse material ($k_d = 0$). (b) Adding bump mapping on top of the underlying surface in order to model the macroscopic appearance of the scales. (c) Replacing the diffuse material with our rough thin-film interference ($\eta_0 = 1$, $\eta_1 = 1.56$, $\eta_2 = 1.0$, $\delta_0 = 900\text{nm}$). (d) Adding an absorption layer ($\sigma_a = 0.7$, $\delta_1 = 2\text{ nm}$, $k_d = 0$) in order to darker the final appearance.

[HHH22] HUANG W., HULLIN M. B., HANIKA J.: A microfacet-based hair scattering model. *Computer Graphics Forum* 41, 4 (2022), 79–91. 2

[HK93] HANRAHAN P., KRUEGER W.: Reflection from layered surfaces due to subsurface scattering. In *Proceedings of the 20th Annual Conference on Computer Graphics and Interactive Techniques* (New York, NY, USA, 1993), SIGGRAPH '93, Association for Computing Machinery, p. 165–174. 2

[HMC*22] HUANG W., MERZBACH S., CALLENBERG C., STAVENGA D., HULLIN M.: Rendering iridescent rock dove neck feathers. In *ACM SIGGRAPH 2022 Conference Proceedings* (New York, NY, USA, 2022), SIGGRAPH '22, Association for Computing Machinery. 2

[IGA15] IGLESIAS-GUITIAN J. A., ALIAGA C., JARABO A., GUTIERREZ D.: A biophysically-based model of the optical properties of skin aging. *Computer Graphics Forum* 34, 2 (2015), 45–55. 2

[JAG18] JARABO A., ALIAGA C., GUTIERREZ D.: A radiative transfer framework for spatially-correlated materials. *ACM Trans. Graph.* 37, 4 (jul 2018). 2

[Jak14] JAKOB W.: <https://www.mitsuba-renderer.org/>, 2014. 4

[JAM*10] JAKOB W., ARBREE A., MOON J. T., BALA K., MARSCHNER S.: A radiative transfer framework for rendering materials with anisotropic structure. *ACM Trans. Graph.* 29, 4 (jul 2010). 2

[JdJM14] JAKOB W., D'EON E., JAKOB O., MARSCHNER S.: A comprehensive framework for rendering layered materials. *ACM Transactions on Graphics* (2014). 2

[KG12] KLEIN M.-C. G., GORB S. N.: Epidermis architecture and material properties of the skin of four snake species. 3

[MJC*03] MARSCHNER S. R., JENSEN H. W., CAMMARANO M., WORLEY S., HANRAHAN P.: Light scattering from human hair fibers. *ACM Transactions on Graphics (TOG)* 22, 3 (2003), 780–791. 2

[MMS12] MAIA R., MACEDO R. H. F., SHAWKEY M. D.: Nanostructural self-assembly of iridescent feather barbules through depletion

- attraction of melanosomes during keratinization. *Journal of the Royal Society, Interface* 9, 69 (April 2012), 734–743. [1](#)
- [MOK*16] MCNAMARA M., ORR P., KEARNS S., ALCALÁ L., ANADÓN P., PEÑALVER E.: Reconstructing carotenoid-based and structural coloration in fossil skin. *Current Biology* 26, 8 (2016), 1075–1082. [1](#)
- [NGH*18] NOVÁK J., GEORGIEV I., HANIKA J., KRIVÁNEK J., JAROSZ W.: Monte carlo methods for physically based volume rendering. In *ACM SIGGRAPH 2018 Courses* (New York, NY, USA, 2018), SIGGRAPH '18, Association for Computing Machinery. [2](#)
- [SD17] SHAWKEY M. D., D'ALBA L.: Interactions between colour-producing mechanisms and their effects on the integumentary colour palette. *Philosophical Transactions of the Royal Society B: Biological Sciences* 372, 1724 (2017), 20160536. [2](#)
- [SM92] SMITS B. E., MEYER G. W.: *Newton's Colors: Simulating Interference Phenomena in Realistic Image Synthesis*. Springer Berlin Heidelberg, Berlin, Heidelberg, 1992, pp. 185–194. [2](#)
- [Sta99] STAM J.: Diffraction shaders. In *Proceedings of the 26th Annual Conference on Computer Graphics and Interactive Techniques* (USA, 1999), SIGGRAPH '99, ACM Press/Addison-Wesley Publishing Co., p. 101–110. [2](#)
- [sta20] STACEY: White lipped python care, diet, habitat setup and more for beginners, 2020. [1](#)
- [Sun06] SUN Y.: Rendering biological iridescences with rgb-based renderers. *ACM Trans. Graph.* 25, 1 (jan 2006), 100–129. [2](#)
- [SY21] STEINBERG S., YAN L.-Q.: A generic framework for physical light transport. *ACM Transactions on Graphics (TOG)* 40, 4 (2021), 1–20. [5](#)
- [WW07] WEIDLICH A., WILKIE A.: Arbitrarily layered micro-facet surfaces. In *Proceedings of the 5th International Conference on Computer Graphics and Interactive Techniques in Australia and Southeast Asia* (New York, NY, USA, 2007), GRAPHITE '07, Association for Computing Machinery, p. 171–178. [2](#)
- [Yeh05] YEH P.: *Optical waves in layered media*. Wiley, 2005. [3](#)
- [YHW*18] YAN L.-Q., HAŠAN M., WALTER B., MARSCHNER S., RAMAMOORTHI R.: Rendering specular microgeometry with wave optics. *ACM Transactions on Graphics (TOG)* 37, 4 (2018), 1–10. [2](#)
- [Yos05] YOSHIOKA S. K. S.: Structural colors in nature the role of regularity and irregularity in the structure. [2](#)
- [YTJR15] YAN L.-Q., TSENG C.-W., JENSEN H. W., RAMAMOORTHI R.: Physically-accurate fur reflectance: Modeling, measurement and rendering. *ACM Transactions on Graphics (TOG)* 34, 6 (2015), 1–13. [2](#)
- [ZJ18] ZELTNER T., JAKOB W.: The layer laboratory: A calculus for additive and subtractive composition of anisotropic surface reflectance. *Transactions on Graphics (Proceedings of SIGGRAPH)* 37, 4 (July 2018), 74:1–74:14. [2](#)